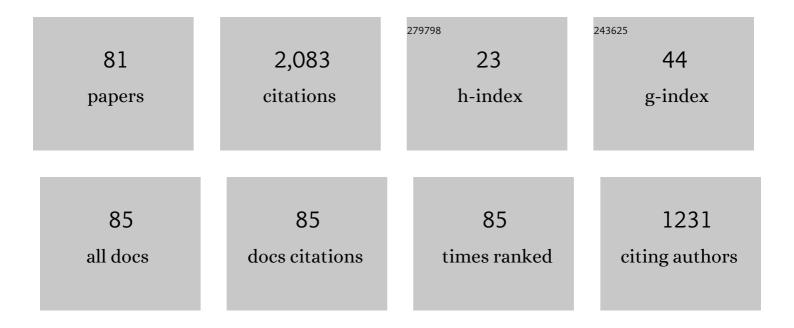
List of Publications by Year in descending order

Source: https://exaly.com/author-pdf/2358235/publications.pdf Version: 2024-02-01



IANCHOON SEO

#	Article	IF	CITATIONS
1	Effect of finite aspect ratio on the neoclassical ion thermal conductivity in the banana regime. Physics of Fluids, 1982, 25, 1493.	1.4	204
2	Numerical study of neoclassical plasma pedestal in a tokamak geometry. Physics of Plasmas, 2004, 11, 2649-2667.	1.9	158
3	On the validity of the local diffusive paradigm in turbulent plasma transport. Physical Review E, 2010, 82, 025401.	2.1	155
4	Effect of impurity particles on the finite-aspect ratio neoclassical ion thermal conductivity in a tokamak. Physics of Fluids, 1986, 29, 3314.	1.4	140
5	Review of deuterium–tritium results from the Tokamak Fusion Test Reactor. Physics of Plasmas, 1995, 2, 2176-2188.	1.9	89
6	Spontaneous rotation sources in a quiescent tokamak edge plasma. Physics of Plasmas, 2008, 15, .	1.9	86
7	Compressed ion temperature gradient turbulence in diverted tokamak edge. Physics of Plasmas, 2009, 16, .	1.9	80
8	A fast low-to-high confinement mode bifurcation dynamics in the boundary-plasma gyrokinetic code XGC1. Physics of Plasmas, 2018, 25, .	1.9	79
9	Plasma transport in stochastic magnetic field caused by vacuum resonant magnetic perturbations at diverted tokamak edge. Physics of Plasmas, 2010, 17, .	1.9	76
10	X-transport: A baseline nonambipolar transport in a diverted tokamak plasma edge. Physics of Plasmas, 2002, 9, 3884-3892.	1.9	73
11	Fast Low-to-High Confinement Mode Bifurcation Dynamics in a Tokamak Edge Plasma Gyrokinetic Simulation. Physical Review Letters, 2017, 118, 175001.	7.8	73
12	ISABELA for effective in situ compression of scientific data. Concurrency Computation Practice and Experience, 2013, 25, 524-540.	2.2	62
13	Property of an X-point generated velocity-space hole in a diverted tokamak plasma edge. Physics of Plasmas, 2004, 11, 5626-5633.	1.9	42
14	A Fokker-Planck-Landau collision equation solver on two-dimensional velocity grid and its application to particle-in-cell simulation. Physics of Plasmas, 2014, 21, .	1.9	36
15	Kinetic neoclassical transport in the H-mode pedestal. Physics of Plasmas, 2014, 21, .	1.9	34
16	Bootstrap current for the edge pedestal plasma in a diverted tokamak geometry. Physics of Plasmas, 2012, 19, .	1.9	31
17	Anisotropic distribution function of minority tail ions generated by strong ionâ€eyclotron resonance heating. Physics of Fluids B, 1990, 2, 310-317.	1.7	29
18	Anomalous losses of deuterium–deuterium fusion products in the Tokamak Fusion Test Reactor*. Physics of Plasmas, 1994, 1, 1469-1478.	1.9	29

JANGHOON SEO

#	Article	IF	CITATIONS
19	Temperature anisotropy in a cyclotron resonance heated tokamak plasma and the generation of poloidal electric field. Physics of Plasmas, 1995, 2, 2044-2054.	1.9	29
20	Pedestal and edge electrostatic turbulence characteristics from an XGC1 gyrokinetic simulation. Plasma Physics and Controlled Fusion, 2017, 59, 105014.	2.1	28
21	Deuterium–tritium plasmas in novel regimes in the Tokamak Fusion Test Reactor. Physics of Plasmas, 1997, 4, 1714-1724.	1.9	27
22	Exploring Data Staging Across Deep Memory Hierarchies for Coupled Data Intensive Simulation Workflows. , 2015, , .		26
23	Cross-verification of the global gyrokinetic codes GENE and XGC. Physics of Plasmas, 2018, 25, 062308.	1.9	26
24	Gyrokinetic simulation study of magnetic island effects on neoclassical physics and micro-instabilities in a realistic KSTAR plasma. Physics of Plasmas, 2018, 25, .	1.9	24
25	Intrinsic momentum generation by a combined neoclassical and turbulence mechanism in diverted DIII-D plasma edge. Physics of Plasmas, 2014, 21, 092501.	1.9	23
26	Constructing a new predictive scaling formula for ITER's divertor heat-load width informed by a simulation-anchored machine learning. Physics of Plasmas, 2021, 28, .	1.9	22
27	Scaling to 150K cores: Recent algorithm and performance engineering developments enabling XGC1 to run at scale. Journal of Physics: Conference Series, 2009, 180, 012036.	0.4	21
28	Mesh generation for confined fusion plasma simulation. Engineering With Computers, 2016, 32, 285-293.	6.1	18
29	A tight-coupling scheme sharing minimum information across a spatial interface between gyrokinetic turbulence codes. Physics of Plasmas, 2018, 25, 072308.	1.9	17
30	Advancing Fusion with Machine Learning Research Needs Workshop Report. Journal of Fusion Energy, 2020, 39, 123-155.	1.2	17
31	Verification of the global gyrokinetic stellarator code XGC-S for linear ion temperature gradient driven modes. Physics of Plasmas, 2019, 26, .	1.9	15
32	Gyrokinetic understanding of the edge pedestal transport driven by resonant magnetic perturbations in a realistic divertor geometry. Physics of Plasmas, 2020, 27, .	1.9	15
33	Particle Simulation of Neoclassical Transport in the Plasma Edge. Contributions To Plasma Physics, 2006, 46, 496-503.	1.1	14
34	Verification of long wavelength electromagnetic modes with a gyrokinetic-fluid hybrid model in the XGC code. Physics of Plasmas, 2017, 24, 054508.	1.9	14
35	Full-f XGC1 gyrokinetic study of improved ion energy confinement from impurity stabilization of ITG turbulence. Physics of Plasmas, 2017, 24, .	1.9	14
36	Towards Real-Time Detection and Tracking of Spatio-Temporal Features: Blob-Filaments in Fusion Plasma. IEEE Transactions on Big Data, 2016, 2, 262-275.	6.1	13

#	Article	IF	CITATIONS
37	Model for collisional fast ion diffusion into Tokamak Fusion Test Reactor loss cone. Physics of Plasmas, 1994, 1, 3857-3870.	1.9	12
38	Nonlinear global gyrokinetic delta- <i>f</i> turbulence simulations in a quasi-axisymmetric stellarator. Physics of Plasmas, 2020, 27, .	1.9	12
39	Spatial coupling of gyrokinetic simulations, a generalized scheme based on first-principles. Physics of Plasmas, 2021, 28, .	1.9	12
40	Wall intersection of ion orbits induced by fast transport of pedestal plasma over an electrostatic potential hill in a tokamak plasma edge. Physics of Plasmas, 2005, 12, 102501.	1.9	11
41	Energy conservation tests of a coupled kinetic plasma–kinetic neutral transport code. Computational Science & Discovery, 2013, 6, 015006.	1.5	11
42	Development of a Gyrokinetic Particle-in-Cell Code for Whole-Volume Modeling of Stellarators. Plasma, 2019, 2, 179-200.	1.8	11
43	Comparative collisionless alpha particle confinement in stellarator reactors with the XGC gyrokinetic code. Physics of Plasmas, 2019, 26, 032506.	1.9	11
44	Study of up–down poloidal density asymmetry of high- impurities with the new impurity version of XGCa. Journal of Plasma Physics, 2019, 85, .	2.1	10
45	Spatial core-edge coupling of the particle-in-cell gyrokinetic codes GEM and XGC. Physics of Plasmas, 2020, 27, 122510.	1.9	10
46	Kinetic modeling of divertor heat load fluxes in the Alcator C-Mod and DIII-D tokamaks. Physics of Plasmas, 2015, 22, .	1.9	9
47	First coupled GENE–XGC microturbulence simulations. Physics of Plasmas, 2021, 28, 012303.	1.9	9
48	Encoder–decoder neural network for solving the nonlinear Fokker–Planck–Landau collision operator in XGC. Journal of Plasma Physics, 2021, 87, .	2.1	9
49	What happens to full-f gyrokinetic transport and turbulence in a toroidal wedge simulation?. Physics of Plasmas, 2017, 24, .	1.9	7
50	Investigation of the plasma shaping effects on the H-mode pedestal structure using coupled kinetic neoclassical/MHD stability simulations. Physics of Plasmas, 2017, 24, .	1.9	7
51	Gyroaveraging operations using adaptive matrix operators. Physics of Plasmas, 2018, 25, .	1.9	7
52	Cross-verification of neoclassical transport solutions from XGCa against NEO. Physics of Plasmas, 2019, 26, .	1.9	7
53	Verification of a fully implicit particle-in-cell method for the v â^¥-formalism of electromagnetic gyrokinetics in the XGC code. Physics of Plasmas, 2021, 28, 072505.	1.9	7
54	Strong variation of average ion energy in oscillation frequency of sheath potential. Physics of Plasmas, 2000, 7, 766-769.	1.9	6

#	Article	IF	CITATIONS
55	Persistent Data Staging Services for Data Intensive In-situ Scientific Workflows. , 2016, , .		6
56	Tokamak ITG-KBM transition benchmarking with the mixed variables/pullback transformation electromagnetic gyrokinetic scheme. Physics of Plasmas, 2021, 28, 034501.	1.9	6
57	Effects of light impurities on zonal flow activities and turbulent thermal transport. Physics of Plasmas, 2022, 29, .	1.9	6
58	POSTER: Leveraging deep memory hierarchies for data staging in coupled data-intensive simulation workflows. , 2014, , .		5
59	Reduction of blob-filament radial propagation by parallel variation of flows: Analysis of a gyrokinetic simulation. Physics of Plasmas, 2020, 27, .	1.9	5
60	Variational calculation of alphaâ€driven bootstrap current in a deutrium–tritium tokamak reactor. Physics of Plasmas, 1996, 3, 3732-3744.	1.9	4
61	Analysis of equilibrium and turbulent fluxes across the separatrix in a gyrokinetic simulation. Physics of Plasmas, 2018, 25, 072306.	1.9	4
62	Comparison of edge turbulence characteristics between DIII-D and C-Mod simulations with XGC1. Physics of Plasmas, 2020, 27, .	1.9	4
63	Feasibility experiments for electron ripple injection on current drive experiment-upgrade. Physics of Plasmas, 1998, 5, 966-972.	1.9	3
64	Numerical study of the plasma wall-bias effect on the ion flux through acceleration grid hole. Physics of Plasmas, 2010, 17, 073505.	1.9	3
65	X-point ion orbit physics in scrape-off layer and generation of a localized electrostatic potential perturbation around X-point. Physics of Plasmas, 2019, 26, 014504.	1.9	3
66	Implementation of higher-order velocity mapping between marker particles and grid in the particle-in-cell code XGC. Journal of Plasma Physics, 2021, 87, .	2.1	3
67	Development of a gyrokinetic hyperbolic solver based on discontinuous Galerkin method in tokamak geometry. Computer Physics Communications, 2022, 273, 108265.	7.5	3
68	Neoclassical transport coefficients for tokamaks with beanâ€shaped flux surfaces. Physics of Fluids B, 1991, 3, 395-399.	1.7	2
69	In Situ Analysis and Visualization of Fusion Simulations: Lessons Learned. Lecture Notes in Computer Science, 2018, , 230-242.	1.3	2
70	A Co-Design Study Of Fusion Whole Device Modeling Using Code Coupling. , 2019, , .		2
71	Verification of an improved equation-free projective integration method for neoclassical plasma-profile evolution in tokamak geometry. Physics of Plasmas, 2020, 27, 032505.	1.9	2
72	A new hybrid simulation model for tokamak plasma turbulence. Computer Physics Communications, 2021, 258, 107626.	7.5	2

#	Article	IF	CITATIONS
73	A Framework for International Collaboration on ITER Using Large-Scale Data Transfer to Enable Near-Real-Time Analysis. Fusion Science and Technology, 2021, 77, 98-108.	1.1	2
74	Computational Knowledge for Toroidal Confinement Physics: Part I. , 2009, , .		1
75	Molecular dynamics simulation of hyperthermal neutrals generated by energetic ion impact on a metal plate. Journal of Applied Physics, 2010, 107, 013304.	2.5	1
76	Improving Gyrokinetic Field Solvers toward Whole-Volume Modeling of Stellarators. Plasma and Fusion Research, 2021, 16, 2403054-2403054.	0.7	1
77	Toward the core-edge coupling of delta-f and total-f gyrokinetic models. Physics of Plasmas, 2022, 29, 032301.	1.9	1
78	Effect of poloidal electric field on electron cyclotron current drive in a tokamak geometry. Physics of Plasmas, 2000, 7, 4948-4959.	1.9	0
79	Finding Structure in Large Data Sets of Particle Distribution Functions Using Unsupervised Machine Learning. IEEE Transactions on Plasma Science, 2020, , 1-4.	1.3	Ο
80	Property of neoclassical GAMs induced by pellet generated plasma perturbations in the gyrokinetic code XGC. Physics of Plasmas, 2021, 28, 044501.	1.9	0
81	Nonlinear Fokker-Planck collision operator in Rosenbluth form for gyrokinetic simulations using discontinuous Galerkin method. Computer Physics Communications, 2022, 279, 108459.	7.5	0